The University of New South Wales Renewable Hydrogen for Export

Research and Development Project

Waste Biomass to Renewable Hydrogen

Project number: 2018/RND015

End of Activity Report

Funded under the Renewable Hydrogen for Export Program

by the Australian Renewable Energy Agency

Authors: A/Prof Jason Scott; Prof Dawei Wang; A/Prof Robert Taylor; Prof Yansong Shen

Key Contributors: Dr Qiyuan Li; Dr Lixue Jiang; Dr Yuting Zhuo, Dr Nicholas Bedford; Ms Yuwei Yang; Dr William Hadinata Lie, Prof Rose Amal

Finalised December 2022

Contents

Executive Summary

The Activity systematically developed a multi-step, solar-driven biomass reforming system capable of extracting hydrogen and/or hydrogen carriers from waste biomass, progressing the technology from TRL3 to TRL4. This document describes the outcomes from the research conducted over the duration of the Activity.

The established biomass reforming system comprises three primary components, which were developed independently and integrated in the final year of the Activity: (i) a waste biomass concentrator (WBC), which is powered by a photovoltaic module to concentrate the biomass feed stream and simultaneously produce clean water suited for use in the downstream flow electrolysis cell; (ii) a solar-thermal biomass pre-treatment reactor (BPR), which contained a solar concentrator and a pressurized thermochemical reactor tube, to pre-condition the biomass to be more appropriate for hydrogen generation; and (iii) a flow electrolysis cell (FEC), which uses a photovoltaic module to convert the BPR output in the anodic compartment along with clean water (from the WBC) in the cathodic compartment to produce hydrogen and value-added organic product.

Experimentally, the integrated prototype system was able to produce 96 L H_2 per day (0.067 L H_2/min) from 25 L/day of waste sugar feedstock (~5 g/L sugar concentration). The results indicate that by scaling the prototype up by 100X, the system could transform 2.5m^3/day of sugar-containing wastewater into 0.85kg/day of renewable hydrogen, along with > 2m^3 clean water and ~1kg/day of valuable by-products (e.g., FDCA). Other key performance metrics of the system were found to be:

(i) A maximum ~58% solar energy conversion to heat and electricity;
(ii) A > 95% waste sugar recovery from the wastewater and < 10kWh/m^3 energy consumption for clean water production;
(iii) An energy consumption of 40-54 kWh/kg hydrogen for biomass electrolysis. Importantly, this is 15% more efficient than for standard water splitting;
(iv) A FDCA yield of up to 87 % from 5-HMF oxidation within the FEC.

Further, a computational fluid dynamic (CFD) model was developed for the BPR and FEC components. After validation, the model was able to:

(i) predict the fundamental physics and chemistry phenomena occurring within each unit;
(ii) assess design variations and identify the operating conditions giving best performance;
(iii) evaluate the performance of scaled-up systems.

Achievement of Milestones. Importantly, the Activity successfully achieved all the technical milestones (as planned and within budget) regarding the delivery of a scaled-up, working prototype tandem biomass reforming system as well as the milestones regarding CFD modelling of the key components.

Outputs/Impact. The project (to date) has generated four journal publications with another four in preparation. Looking forward, a new industry connection which is intending to progress the technology from TRL4 to TRL6 and use it to generate renewable hydrogen from organic-containing waste streams in remote communities, has originated from the Activity.

Abbreviations and Acronyms

ARENA	Australian Renewable Energy Agency
AUD	Australian Dollars
B.O.W.	Beijing Origin Water
BPR	Biomass Pre-treatment Reactor
CdTe	Cadmium Telluride
CEO	Chief Executive Officer
CFD	Computational Fluid Dynamics
COD	Chemical Oxygen Demand
CPC	Concentrated Parabolic Collector
CSIRO	Commonwealth Scientific and Industrial Research Organisation
DC	Direct Current
FE	Faradaic Efficiency
FEC	Flow Electrolyser Cell
HER	Hydrogen Evolution Reaction
KOH	Potassium Hydroxide
LA	Levulinic Acid
LNG	Liquified Natural Gas
NiMo	Nickel Molybdenum
NSW	New South Wales
OD	Outer Diameter
OER	Oxygen Evolution Reaction
PV	Photovoltaic
RO	Reverse Osmosis
TOC	Total Organic Carbon
TRL	Technology Readiness Level
UNSW	University of New South Wales
UV	Ultraviolet
WBC	Waste Biomass Concentrator
2,5-FDCA	2,5-Furandicarboxylic acid
3D	3 Dimensional
3MT	3 Minute Thesis
5-HMF	5-Hydroxymethylfurfural

1. Introduction

1.1 Context

A richness of resources in Australia have seen it be a significant energy exporter to other nations. For instance, in 2021, natural gas (LNG) exports from Australia were ~$50 billion AUD. Increasingly though, many countries are seeking to transition away from fossil-fuel derived energy sources to sustainable alternatives, such as renewable hydrogen, however they do not necessarily have the capacity to do so. Given the ongoing shift in the global energy landscape, opportunity exists for Australia to remain a strong energy exporter by contributing to the expansion of renewable (solar) hydrogen into the global energy market. Consequently, there is considerable interest in producing H_2 from electrochemical water splitting in a feasible yet sustainable way for worldwide distribution. While water is known as a renewable and abundant resource, its use as a H_2 source is relatively energy intensive (>4.5 kWh m_{H2}^{-3}), is subject to competing uses (e.g., drinking water, agriculture) and is reasonably costly (i.e., the water oxidation reaction is sluggish). These are the key reasons as to why there is a strong urge to develop unique systems to improve the process efficiency, one of which is to use a waste biomass stream in place of water as a feedstock for the electrolyser.

Traditionally, biomass is used to produce syngas by reforming and gasification. Turning to biomass as a H_2 source in an electrolytic system has many advantages, from energy to economic benefits. Biomass can be produced at very low cost from raw biomass streams (e.g., sugars and vegetable oils in waste) and they generally have a very low standard oxidation potential (< 0.2V) compared to water oxidation (1.23V). Biomass oxidation by electrochemical means is selective and scalable, delivers zero CO_2 emissions and has the added advantage of producing value-added organic products from the process.

1.2 Objectives

The Activity aimed to develop a biomass reforming system capable of extracting hydrogen and/or hydrogen carriers, such as bio-alcohols and bio-acids, from waste biomass. The biomass reforming system comprises a biomass pre-conditioning reactor (BPR) coupled with a flow electrolyser cell (FEC) to produce renewable H_2 without any CO_2 emissions. Final deliverables projected for the Activity were to:

i) Optimise the original laboratory-scale FEC system, develop a suitable electrocatalyst and procure and optimise a laboratory-scale BPR;
ii) Scale-up the BPR (50 mL/min semi-continuous capacity) and FEC (0.5-1 L capacity) components of the system so as to be operational outdoors. This included adaptation of a solar concentrator evacuated tube array to the BPR component and adaptation of a photovoltaic (PV) cell to the FEC component;
iii) Integrate the FEC and BPR units to give the tandem biomass reformer and demonstrate a capacity to produce H_2 from a representative waste biomass stream;
iv) Establish a computational model which can describe BPR and FEC unit performance and be used to guide system scale-up;
v) To progress the technology from TRL3 to TRL4.

This End of Activity Report describes key outcomes from the Activity as well as provides details on lessons learned, commercialisation prospects, knowledge-sharing undertakings and future plans for the technology.

2. Outcomes

2.1 Overview

A stand-alone modular system has been designed, constructed and performance-tested which utilises a waste biomass stream and sunlight to generate hydrogen renewably. A schematic of the system is provided in Figure 1. The system comprises three primary integrated components: (i) a waste biomass concentrator (WBC) powered by a photovoltaic cell which concentrates the biomass feed stream and simultaneously produces clean water suitable for use in the flow electrolysis cell; (ii) a solar-thermal biomass pre-treatment reactor (BPR) which pre-conditions the biomass to be more appropriate for hydrogen generation; and (iii) a flow electrolysis cell (FEC) powered by a photovoltaic cell which uses pre-conditioned biomass in the anodic compartment (from the BPR) and clean water in the cathodic compartment (from the WBC) to produce hydrogen and value-added organic product.

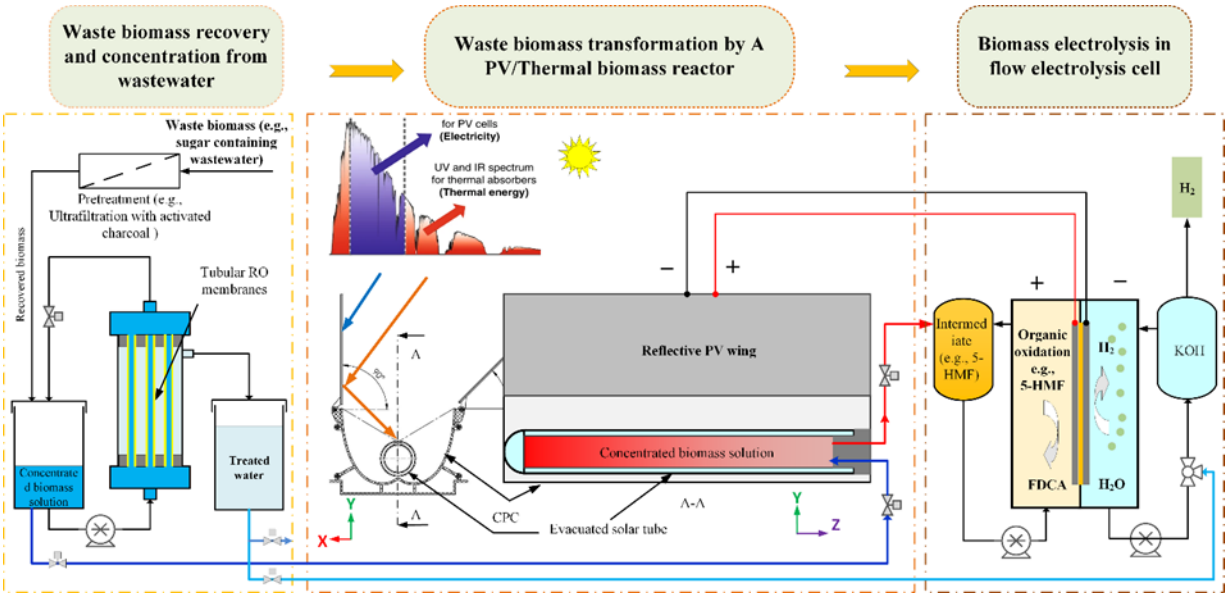

***Figure 1:** Schematic of the tandem system for generating renewable hydrogen from sunlight and a biomass feedstock. The system comprises three components: (i)* waste biomass concentrator *(powered by a photovoltaic cell); (ii) a solar-thermal biomass pre-treatment reactor; (iii) a flow electrolysis cell (powered by a photovoltaic cell).*

Details on the development and performance of each of the components as well as the overall system are provided in the ensuing sections.

2.2 Waste Biomass Concentrator

The Activity aimed to take advantage of waste liquid biomass streams, but such streams must first be recovered, purified, and concentrated. Thus, the first step in our overall process was to develop a solar-driven unit capable upgrading biomass feedstocks for the later components of the system. For instance, a high-sugar-containing waste stream, such as that from the soft drink industry, contains a suite of other organics as well as carbonic acid (i.e., dissolved CO_2), bicarbonates, phosphoric acid, cations (e.g., calcium, sodium) and anions (e.g., Cl) which can impact system performance. To constrain their potentially negative influence on overall system performance a waste biomass concentrator (WBC) has been installed upstream of the

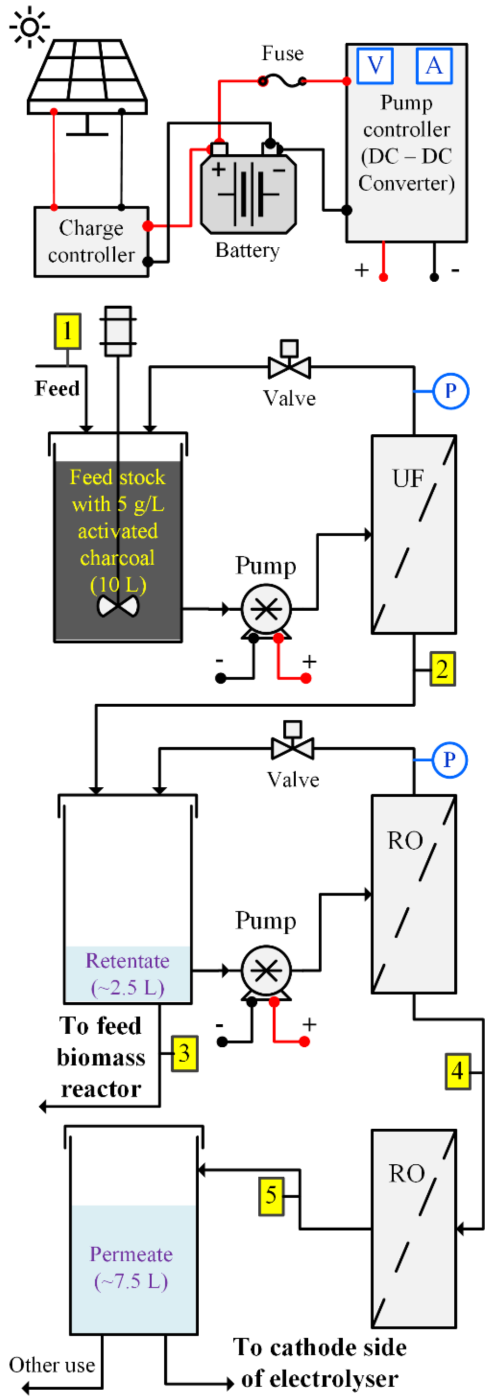

Figure 2: *Schematic depicting configuration of waste biomass concentrator (WBC). The numbers correspond to the x-axis values in Figure 3 below.*

BPR which acts to: (i) decrease their presence in the BPR feed; (ii) concentrate the sugar content of the BPR feed; and (iii) provide a clean water source suitable for use in the cathodic compartment of the FEC.

The WBC comprises: (i) a 5g/L activated charcoal suspension (25°C agitated at 200rpm); (ii) a ceramic ultrafiltration (UF) module (Filtanium Ceramic Membrane, 100KD, 0.004m^2 surface area, 10mm OD x 250mm length); (iii) a primary reverse osmosis module (RO1, PCI Polyamide Thin-Film Composite, 0.2m^2 area, 12.5mm OD × 600mm length, 9 pieces/module); a secondary RO module (RO2, Filmtec TW30HP-4611, Polyamide Thin-Film Composite, 2.0m^2 area/module). The arrangement is shown in Figure 2.

A simulated soft drink wastewater (3% cola, 3.5% apple juice, 3.5% lemonade and 90% water) was prepared and passed through the WBC. The change in key characteristics of the simulated wastewater as it passed through the process is shown in Figure 3. Greater detail on the individual constituents provided in Table A1 (Appendix).

Figure 3 shows that the activated charcoal/UF is effective at removing the coloring components from the wastewater. Importantly, the first RO stage (RO1) is effective at doubling the sugar concentration of the wastewater as well as decreasing the volume of water being fed into the BPR. The increased sugar content and decreased solution volume enable a more economical BPR performance.

The permeate from RO1 contains substantially decreased concentrations of all the initial wastewater characteristics and is suitable as general wash-down water, for irrigation or drinking (following ultraviolet sterilization). A portion of the RO1 permeate is suitable as water supply for the FEC following further purification in RO2 (Figure 3).

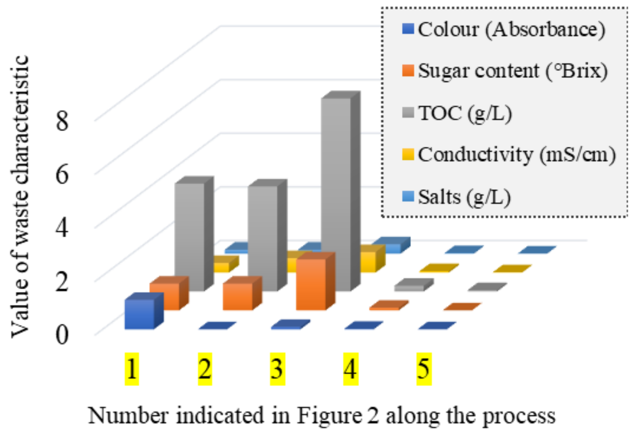

Figure 3: *Change in simulated sugar-containing wastewater characteristics at various points along Waste Biomass Concentrator (WBC) process. Note that [3] is fed to the Biomass Pretreatment Reactor (BPR) and [5] is fed to the cathode compartment of the Flow Electrolysis Cell (FEC)*

2.3 Solar-thermal Biomass Pretreatment Reactor

As detailed in Section 2.2, output [3] from the WBC (Figure 2 and 3), comprising the concentrated biomass product stream, is then fed into the solar-thermal BPR. The prototype solar-thermal BPR comprises an evacuated tubular receiver/reactor which lay along the focal line of a reflective concentrated parabolic collector (CPC). The CPC redirects incident rays from the sun onto the tubular receiver/reactor to provide sufficient heat for the reaction to occur. Additional movable reflective wings were attached to the CPC which facilitate greater sunlight capture during daylight hours (Figure 4a and 4b).

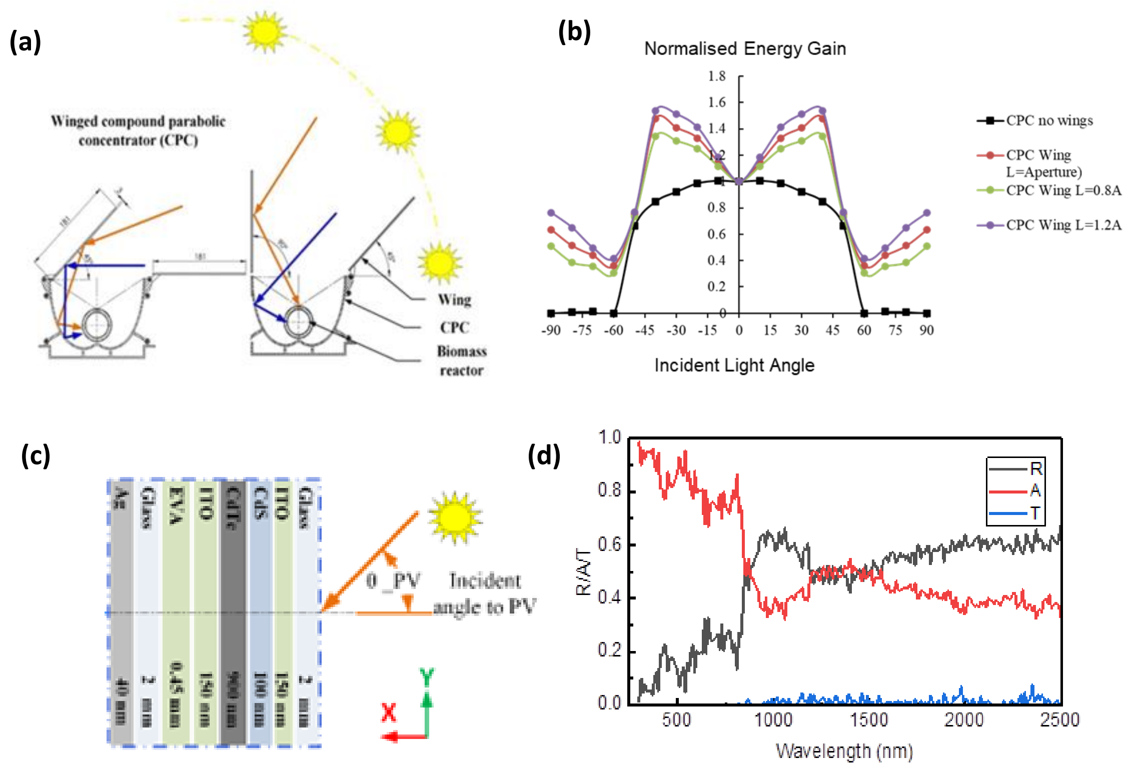

Figure 4: *(a) Schematic of solar-thermal BPR showing position of reflective wings relative to the sun throughout the day; (b) change in normalised energy gain with incident light angle for the concentrated parabolic collector (CPC) with and without reflective wings; (c) cross section of encapsulated CdTe cell (layer thickness not to scale); (d) simulated reflectance, transmission and absorbance of CdTe PV cell on reflective BPR wing at 0° ray incident angle.*

For the hydrogen generated by the system to be completely renewable all energy inputs need to be from the sun. This includes heating via solar-thermal and electrical via photovoltaics (Figure 1). The infra-red portion of the incident sunlight is predominantly responsible for heating the tubular receiver/reactor in the solar-thermal system while the ultra-violet (UV) and visible portions of the spectrum contribute little to this unit and are lost. To broaden usage of the sunlight incident on the BPR to encompass the UV/visible component of the spectrum, cadmium telluride (CdTe) photovoltaic cells were installed on the reflective wings (Figure 4c) which provide power to drive the system components (i.e., FEC and pumps) as well as decrease the system footprint. Optical simulation results for the CdTe solar cell (Figure 4d) showed that the CdTe cell has high absorbance (>70%) in the UV and visible regions (0-700nm wavelength) and lower absorptance (~40%) in infrared region (700-2500nm wavelength), while the UV/visible light reflectance is ~20% and infrared reflectance is over 50%.

The final prototype BPR system (Figure 5a) used a 1.8m long tubular reactor supplied by Apricus Australia (https://apricus.com.au/) with design advice provided by their CEO, Mick Humphries. The tubular reactor is essentially a repurposed evacuated tube collector used in Apricus' solar hot water systems and is commercially available. A stainless-steel reactor was custom designed and fitted within the evacuated tube to protect against release of the reaction fluid (see Section 3.1 below). The current BPR configuration is a batch reactor capable of treating up to 2.5L of reaction fluid at any one time. Experimental tests results (i.e., optical, thermal, stagnation) indicated that the system has an optical efficiency of 60% and a thermal efficiency close to 50% at a temperature of 150°C and a maximum achievable temperature of 320°C. Laboratory-scale studies conducted in the early stages of the project indicated the optimum operating temperature for converting sucrose to 5-hydroxymethylfurfural (5-HMF, the targeted compound to be fed into the FEC) was 150°C which was confirmed by outdoor tests conducted on the prototype unit (Figure 5b). In this instance the maximum attainable 5-HMF yield was 30mol% representing a concentration of ~7.5g 5-HMF/L in the final product stream (feed into the FEC).

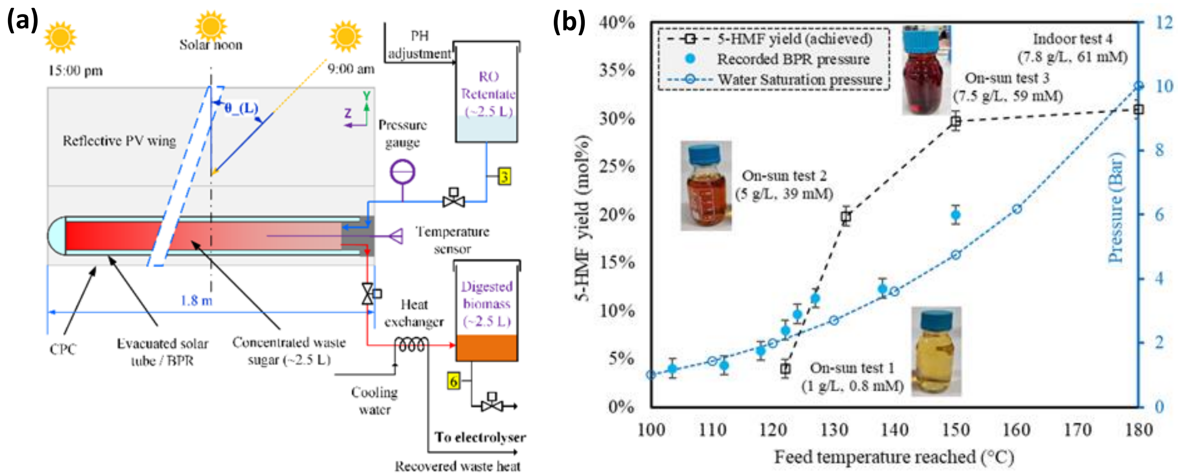

Figure 5: *(a) Schematic of BPR components in the tandem system; (b) results from 'on-sun' testing of the PV winged-BPR using a sucrose feedstock. Initial sucrose concentration = 0.1 Mol; initial feedstock pH = 1.3 (sulfuric acid); reaction volume 2.5 L. Global radiation 850 +/- 100 W/m^2, diffuse radiation: 80+/-10 W/m^2, ambient temperature: 20 +/- 3°C.*

Following treatment in the BPR, the preconditioned sugar stream is stored in a holding tank where it is can then be drawn upon as the feedstock for the FEC.

2.4 Flow Electrolyser Cell

As detailed in Section 2.2 and Section 2.3, output [5] from the WBC (Figure 2 - comprising the clean water) and the pre-conditioned biomass from the BPR (Figure 5) are then fed into the FEC cathode and anode, respectively. The prototype FEC (Figure 6a) comprised a 7.9cm x 7.9cm electrode array with the bias provided by a battery charged by a PV cell (regulated using a DC-DC power regulator). The outdoor prototype set-up is shown in Figure 6b and the corresponding schematic in Figure 6c.

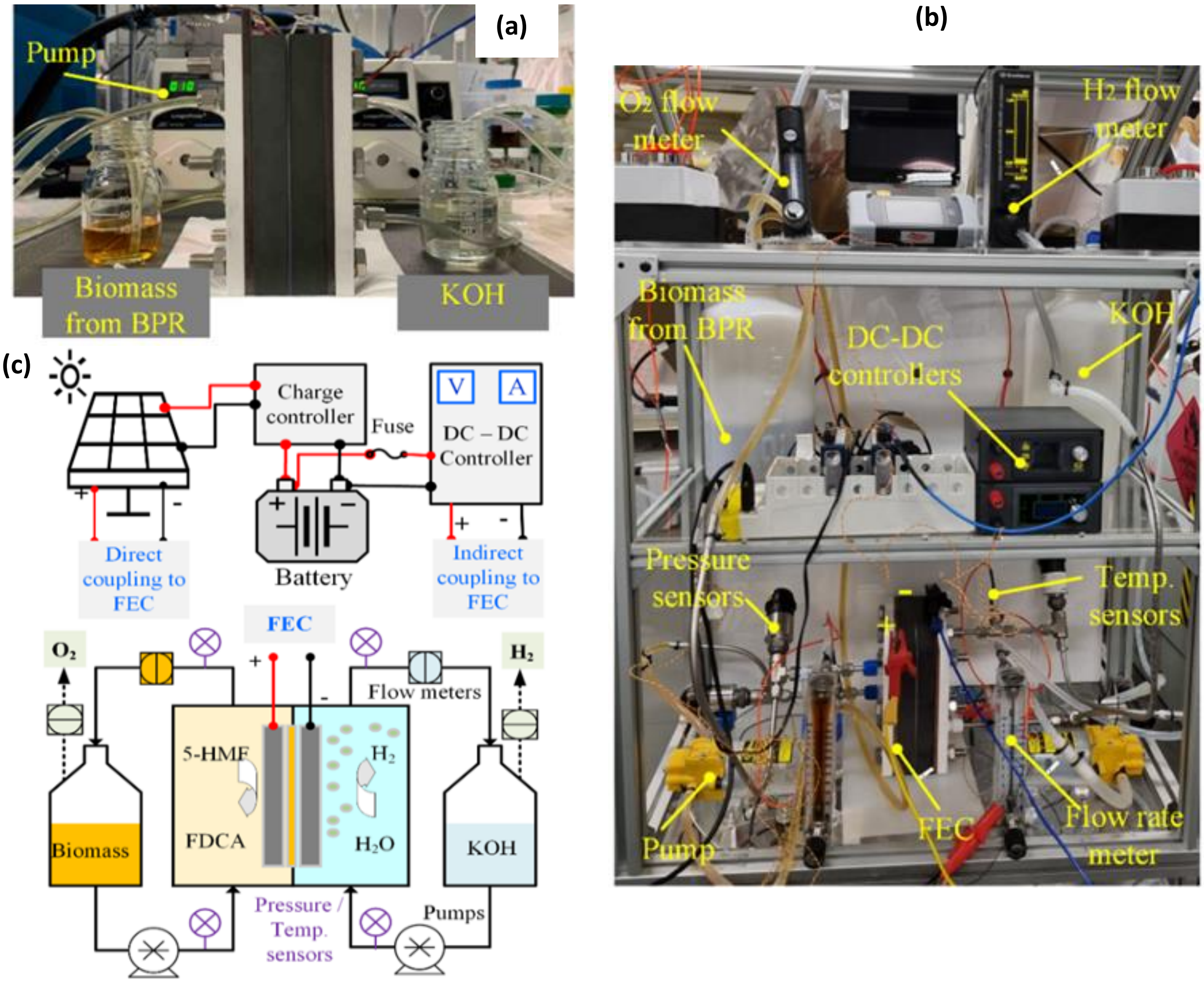

Figure 6: *(a) Image showing FEC with pretreated sugar solution (from the BPR) passing through the anodic compartment (left) and water through the cathodic compartment (right); (b) image showing FEC components of outdoor prototype array; (c) schematic depicting the FEC components of the tandem system.*

Two electrode materials were examined for use within the FEC unit: (i) conventional Ni foam and (ii) conventional Ni foam with (in-house) NiMo coated on its surface. A comparison of the performance of the two electrodes is provided in Table 1. In the case of traditional water splitting (1M KOH electrolyte (anode)), the NiMo electrode was 20.3% more energy efficient at a 10 mA/cm^2 current density (9.2% more energy efficient at a 100 mA/cm^2 current density).

Adding 50mM of 5-HMF to the 1M KOH electrolyte for the NiMo electrode sees a further 17.3% increase in energy efficiency at a 10 mA/cm^2 current density (negligible additional benefit at a 100 mA/cm^2 current density). Using 50mL of the BPR solution as the electrolyte (with 1M KOH) for the NiMo electrode results in a slightly lower improvement in energy efficiency (15.8%) compared to the 50mM 5-HMF at a 10 mA/cm^2 current density while at 100 mA/cm^2 current density there is a 9.9% improvement over the water splitting case. Note that the current density corresponds directly to the rate of hydrogen generation.

Table 1: *Performance comparison by FEC using different electrode materials (Ni foam and in-house NiMo) and electrolyte solutions ((i) 1M KOH (water splitting); (ii) 50 mM 5-HMF +1 M KOH and (iii) BPR solution +1 M KOH).*

Electrolyser type	**Ni electrodes**		**NiMo electrodes**					
Temperature (°C)	25		25		25		25	
Electrolyte	1 M KOH		1 M KOH		50 mM 5-HMF +1 M KOH		BPR solution +1 M KOH	
Products	H_2		H_2		H_2		H_2	
	O_2		O_2		FDCA (85% yield)		FDCA (20% yield)	
Current density (mA cm^{-2})	10	100	10	100	10	100	10	100
Cell voltage (V)	2.1	2.4	1.76	2.2	1.5	2.2	1.52	2
Energy consumption (kWhkg^{-1} of H_2)	56.3	64.4	46.8	59.0	39.9	59.0	40.4	53.7

2.5 Integrated System

The overarching aim of the Activity was to produce a working integrated prototype array which combined the individual unit operations and was able to produce renewable hydrogen from a waste biomass stream. The second half of the the Activity focussed on integrating the units and performance testing the combined system. Images of the final commissioned prototype system are provided in Figure 7, illustrating the positioning of the WBC, BPR and the FEC. Overall, the tandem unit has a 2.0m x 0.8m x 1.8m footprint

A summary of the key performance indicators by the prototype system, configured to include concentration of the sugar feedstock in the WBC, the PV/solar-thermal BPR, and NiMo alloy-containing FEC were found to be:

(v) A maximum ~58% solar energy can be converted to heat and electricity (50% solar to thermal efficiency at 150°C and ~ 8% PV efficiency);
(vi) A > 95% of waste sugar can be recovered from the wastewater and <10 kWh/m^3 energy consumption for clean water production;
(vii) An energy consumption of 40-54 kWh/kg of hydrogen is achievable by biomass electrolysis using the NiMo catalyst, which is 15% more efficient than traditional water splitting using a Ni foam electrocatalyst;
(viii) A 2,5-FDCA yield of up to 87 % can be achieved from the 5-HMF oxidation process within the FEC with ~99% Faradaic Efficiency (FE) delivered for hydrogen evolution. The high FE indicates the actual measured amount of hydrogen produced is very close to the theoretical amount whereby negligible unwanted side reactions occur;

(ix) Overall, the prototype system can produce 96 L H_2 per day (0.067 L H_2/min) from 25 L/day of waste sugar feedstock (~5 g/L sugar concentration). The results indicate that 100 times scaling up of the current prototype will enable transformation of 2.5m^3/day of sugar-containing wastewater to 0.85kg/day renewable hydrogen, > 2m^3 clean water and valuable by-products (e.g., 1 kg/day 2,5-FDCA).

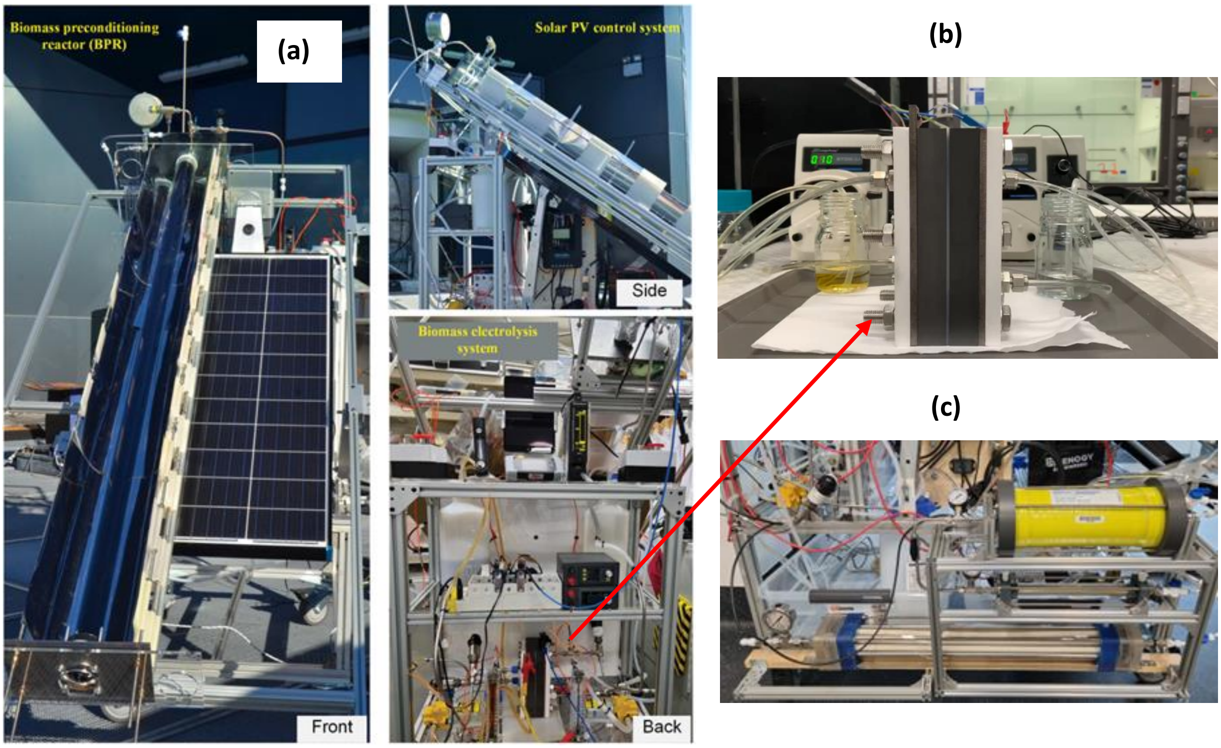

Figure 7: *Images of: (a) rooftop tandem prototype array showing (left) front view, (right top) side view and (right bottom) rear view; (b) close-up of FEC cell; (c) waste biomass concentration system.*

2.6 CFD Modelling

As a part of the Activity, CFD modelling was conducted to examine the thermochemical behaviour of the BPR and water-splitting in the FEC. The numerical models developed for the BPR and FEC were validated using experimental data and then used to improve phenomena occurring within each unit, optimise component configuration and provide a tool which can assist with future scale-up of the system. Detail on the models developed for the BPR and FEC are provided in the ensuing sub-sections.

2.6.1 BRP Modelling

A 2D transient multiphase flow CFD model was developed to describe the HMF production-related heat and mass transfer processes in the reactor. Based on the Euler-Euler approach, a transient gas-liquid multiphase reacting flow model was developed to describe the interpenetrating continua phases, i.e., gas phase and liquid phase, whose volume fractions were assumed to be continuous fractions in space and time. A set of 3D unsteady-state Reynolds averaged Navier-Stokes equations closed by standard $k - \omega$ turbulence model equations was used to describe the two phases. The heat transfer between gas and liquid and chemical reactions associated with sucrose hydrolysis was taken into consideration. The conservations of mass, momentum, and energy of each phase are shown in Table 2.

***Table 2**: Governing equations of gas and liquid phase.*

Gas phase
$\frac{\partial}{\partial t}(\alpha_g \rho_g Y_i) + \nabla(\alpha_g \rho_g Y_i \vec{v}_g) = \dot{m}_i + S_i$
$\frac{\partial}{\partial t}(\alpha_g \rho_g \vec{v}_g) + \nabla(\alpha_g \rho_g \vec{v}_g \vec{v}_g) = -\alpha_g \nabla P + \nabla \bar{\bar{\tau}}_g + \alpha_g \rho_g \vec{g} + K_{lg}(\vec{v}_l - \vec{v}_g) - \dot{m}_{lg} \vec{v}_{lg}$
$\frac{\partial}{\partial t}(\alpha_g \rho_g h_g) + \nabla(\alpha_g \rho_g \vec{v}_g h_g) = -\alpha_g \frac{\partial P}{\partial t} + \bar{\bar{\tau}}_g : \nabla \vec{v}_g - \nabla \vec{q}_g + S_g + Q_{lg} + \dot{m}_{lg} h_{lg}$
Liquid phase
$\frac{\partial}{\partial t}(\alpha_l \rho_l Y_j) + \nabla(\alpha_l \rho_l Y_j \vec{v}_l) = \dot{m}_j + S_j$
$\frac{\partial}{\partial t}(\alpha_l \rho_l \vec{v}_l) + \nabla(\alpha_l \rho_l \vec{v}_l \vec{v}_l) = -\alpha_l \nabla P - \nabla P_l + \nabla \bar{\bar{\tau}}_l + \alpha_l \rho_l \vec{g} + K_{gl}(\vec{v}_g - \vec{v}_l) - \dot{m}_{lg} \vec{v}_{lg}$
$\frac{\partial}{\partial t}(\alpha_l \rho_l h_l) + \nabla(\alpha_l \rho_l \vec{v}_l h_l) = -\alpha_l \frac{\partial P}{\partial t} + \bar{\bar{\tau}}_l : \nabla \vec{v}_l - \nabla \vec{q}_l + S_l + Q_{gl} - \dot{m}_{lg} h_{lg}$
Energy equation of phase change material
$\frac{\partial}{\partial t}(\rho H) + \nabla(\rho H \vec{v}_l H) = \nabla(k \nabla T) + S$
Momentum sink due to the reduced porosity in the mushy zone
$S = \frac{(1-\beta)^2}{(\beta^2 + \varepsilon)} A_{mush}(\vec{v} - \vec{v}_p)$

In this model, the 5-HMF production-related reactions were modelled based on the multi-step mechanism with the model details of the kinetics data shown in Figure 8.

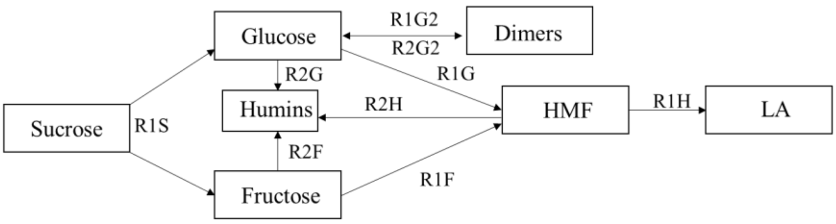

$$C_{H^+} = C_{H_2SO_4} + \frac{1}{2}\left(-K_{a,H_2SO_4^-} - C_{H_2SO_4} + \sqrt{\left(K_{a,H_2SO_4^-} + C_{H_2SO_4}\right)^2 + 4C_{H_2SO_4} K_{a,H_2SO_4^-}}\right)$$

$$K_{1S} = K_{1RS} \exp^{[Ea_{1S}/R(\frac{T-T_R}{T_R T})]}$$

The individual reaction rates expression :
$R_{1S} = k_{1s}(C_{SUC})(C_{H^+})$
$R_{1F} = k_{1F}(C_{FRC})(C_{H^+})$
$R_{2F} = k_{2F}(C_{FRC})(C_{H^+})$
$R_{1G} = k_{1G}(C_{GLC})(C_{H^+})$
$R_{2G} = k_{2G}(C_{GLC})(C_{H^+})$
$R_{1H} = k_{1H}(C_{HMF})(C_{H^+})$
$R_{2H} = k_{2H}(C_{HMF})(C_{H^+})$
$R_{1G_2} = k_{1G_2}(C_{GLC})(C_{H^+})$
$R_{2G_2} = k_{2G_2}(C_{G_2})(C_{H^+})$

Kinetic constants	Value	Unit
k_{1RS}	730±290	$L\ mol^{-1} min^{-1}$
k_{1F}	0.361	$L\ mol^{-1} min^{-1}$
k_{2F}	0.200	$L\ mol^{-1} min^{-1}$
k_{1G}	0.009	$L\ mol^{-1} min^{-1}$
k_{2G}	0.005	$L\ mol^{-1} min^{-1}$
k_{1H}	0.225	$L\ mol^{-1} min^{-1}$
k_{2H}	0.026	$L\ mol^{-1} min^{-1}$
k_{1G_2}	0.227	$L\ mol^{-1} min^{-1}$
k_{2G_2}	1.427	$L\ mol^{-1} min^{-1}$

Activation energy	Value	Unit
Ea_{1s}	110	$kJ\ mol^{-1}$
Ea_{1G}	153	$kJ\ mol^{-1}$
Ea_{2G}	173	$kJ\ mol^{-1}$
Ea_{1F}	116	$kJ\ mol^{-1}$
Ea_{2F}	122	$kJ\ mol^{-1}$
Ea_{1HMF}	92	$kJ\ mol^{-1}$
Ea_{2HMF}	146	$kJ\ mol^{-1}$
Ea_{1G_2}	55	$kJ\ mol^{-1}$
Ea_{2G_2}	99	$kJ\ mol^{-1}$

***Figure 8:** Sucrose reaction model and the related kinetics data.*

In addition to overall experimental performance evaluation, the internal state of the system was assessed using the developed CFD model in terms of temperature and chemical components' evolution. Figure 9a depicts the temperature profile and 5-HMF molar concentration evolution throughout the reaction process. The model predicts that the reaction medium reaches 120 °C after 1.25 hours on-sun and maintains a temperature between 120-150 °C during the next four hours, agreeing well with the experimental data. The 5-HMF evolution predicted by the CFD model also shows reasonable agreement with the experimental results. The comparison demonstrates the capability of the developed CFD model to reasonably predict BPR performance and predict 5-HMF production for the system. Figure 9b shows that while sucrose decomposition into glucose and fructose occurs at the same rate (over the first 30 min), fructose is more readily decomposed into 5-HMF than glucose. This is illustrated by the greater rate of fructose consumption as time progresses. The 5-HMF yield with time is defined by the rate of its production from glucose/fructose in relation to the rate of its subsequent conversion into levulinic acid (LA). As the glucose/ fructose source becomes less available, 5-HMF yield will gradually decrease as its conversion into LA becomes more prevalent. This may account for the decrease in 5-HMF yield with time for the on-sun BPR experiment. The product profiles in Figure 9b indicate that extending the reaction time is not advantageous for 5-HMF yield. Consequently, an appropriate operating strategy is crucial to optimise BPR reactor efficiency and product yield, as well as evaluate cost-effectiveness of the system. The developed CFD model can used to better understand the reactor design and reaction processes as well as guide operating strategy to optimise overall system performance in the future.

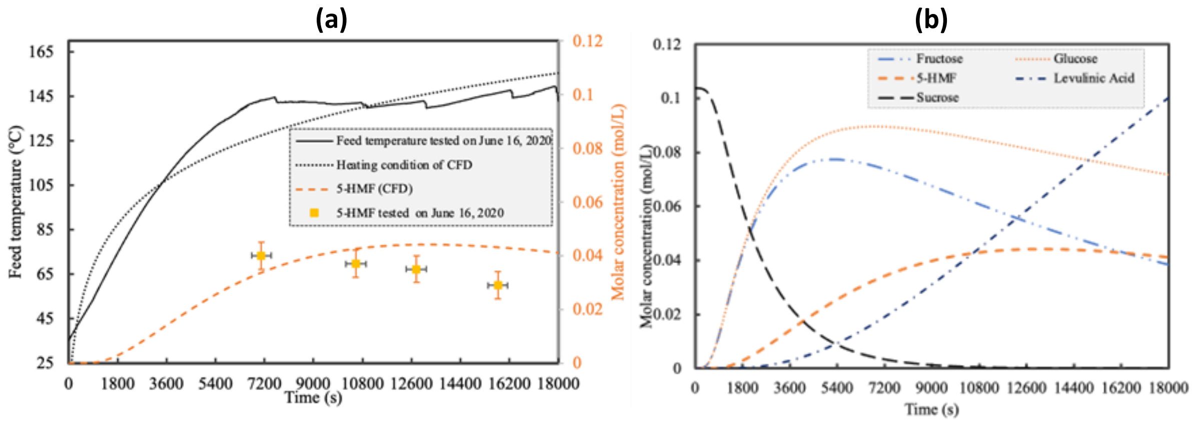

Figure 9: *(a) CFD model prediction of reaction medium temperature and 5-HMF molar concentration evolution of BPR on-sun experiments; (b) Simulation results describing the kinetics of product yield with time during sucrose conversion. Target product is 5-HMF.*

2.6.2 FEC Modelling

A three-dimensional transient CFD model for the laboratory scale FEC has also been developed. In this system, the electrochemical reactions and species separation (e.g., hydrogen) by the membrane has been modelled for the first time (Figure 10). The established model can now be used to understand and optimise the processes in relation to the structure of specific FEC components. For instance, the model can be used to design/tune liquid flow channels to control the bubble resistance thereby improving the electrolysis efficiency.

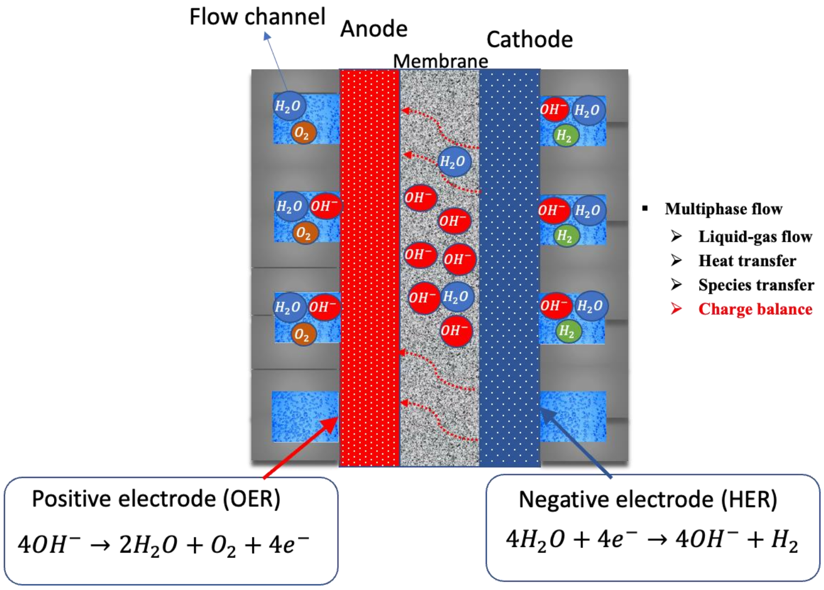

Figure 10: *Mechanistic processes employed for modelling of the FEC unit*

Figure 11 details the internal components of the FEC and the mesh that was generated based on the lab-scale electrolyser prototype. The FEC model was developed based on the Euler-Euler method and coupled with electrolysis-related heat and mass transfers, such that the species transfer between the membrane and the OER and HER reactions which occur on the electrode surface could be simulated.

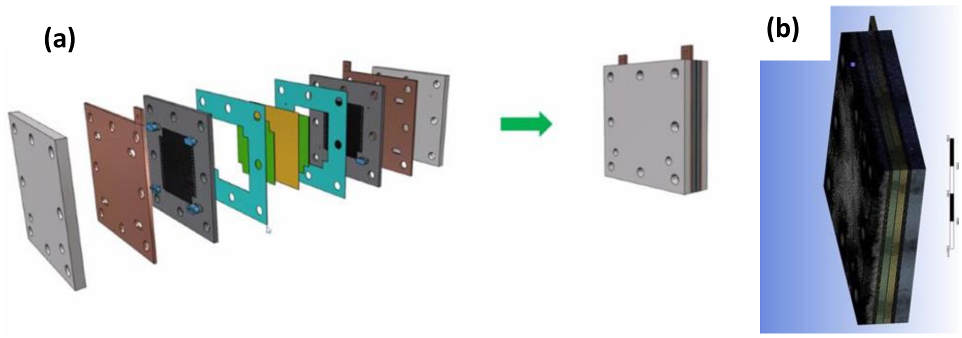

Figure 11: *(a) Arrangement of components within the FEC and (b) the mesh used for CFD modelling of the FEC.*

2.6.2.1 Model Validation

For an FEC, the IV curve reflects its performance. The simulated IV curve from the CFD model was compared with the experimentally measured data, with the appraisal provided in Figure 12. The comparison confirmed the validity and accuracy of the CFD model. The model was then used to perform electrolyser internal state illustrations as well as structure optimisation, which are difficult to achieve via experimental studies alone.

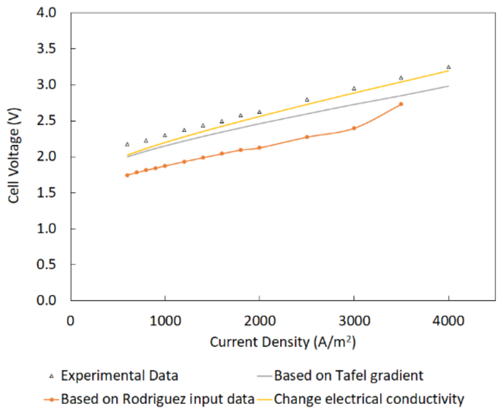

Figure 12: *Comparison between the experimentally measured IV curve and the simulated IV curve for the FEC under the same operating conditions.*

2.6.2.2 Electrolyser Internal State Illustration

Understanding the internal state of the FEC contributes to systematically observing the electrolysis-related flow and heat and mass transfers inside different components of the cell. For example, the evenly distributed potential imposed on the electrode surface and the stable flow field in the flow channel could benefit operation of the FEC. Also, it is necessary to point out that the so-called bubble resistance, i.e., the existence of gas bubbles in the electrolyte, causes the degradation of FEC operating efficiency. Figure 13 shows the hydrogen/oxygen mass fraction distribution in the flow channels, the current potential distribution on the electrode surfaces, the electrolyte flow field, and the bubble formation on the electrode surfaces derived from the CFD modelling. By effectively accessing this information, FEC operating condition and structure tunning can be readily examined through numerical trials.

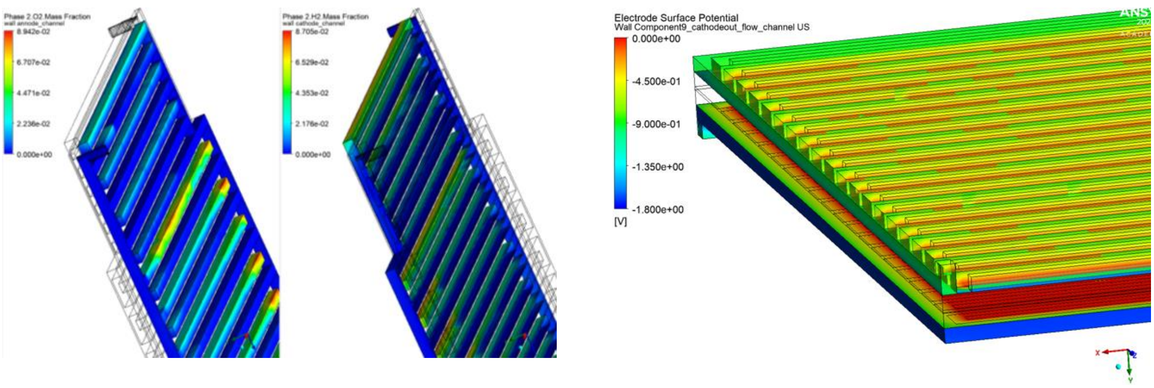

(a) **(b)**

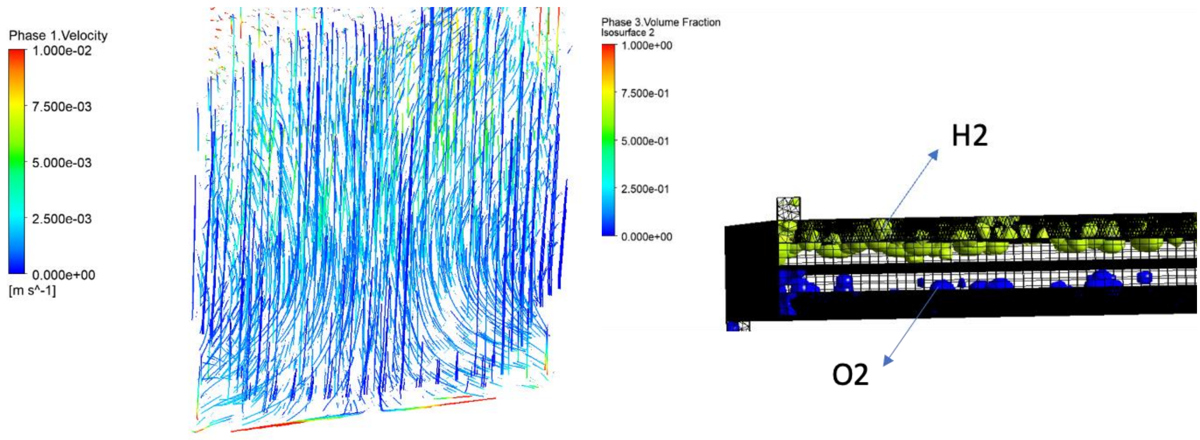

(c) **(d)**

Figure 13: *Selected CFD modelling outputs for the FEC: (a) H_2/O_2 mass fraction distribution in the FEC flow channels; (b) electrical surface potential distribution on the FEC electrodes; (c) electrolyte velocity field within the FEC; (d) gas bubble evolution in the FEC flow channels.*

Using the CFD model, the water-splitting performance could be quantified. Figure 14a shows the simulated gas flow rates that were monitored at the cathode/anode flow channel outlets. It is apparent that, during the initial stage, the flow rate rises quickly and approaches a stable value after 2 mins. The H_2 flow rate is twice that of the O_2 flowrate and stabilizes at this level in the later stages of the electrolysis process. The total gas volume resulting from electrolysis can be quantified (Figure 14b). In general, the developed CFD model can predict hydrogen productivity from water splitting under various operating conditions in the FEC.

(a) **(b)**

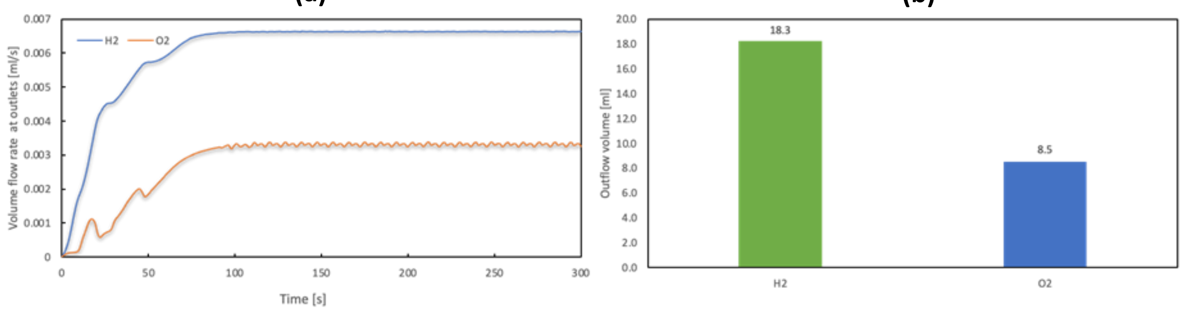

Figure 14: *The CFD-predicted gas volume flow rates at the outlets during electrolysis: (a) volume flow rate of H_2/O_2 at outlets; (b) total volume of produced H_2/O_2 throughout the electrolysis process.*

2.6.2.3 Flow Channel Optimisation

In general, a flow channel with a higher bubble removal rate will exhibit a higher pressure drop. Optimising the flow channel design is always strived by researchers to balance the bubble removal efficiency and the pressure drop. To improve the bubble removal efficiency and reduce the bubble resistance, an optimised flow channel design for the FEC has been established and numerically examined. The ideal flow configuration identified by the model combines both single serpentine and parallel flow characteristics to increase the electrolyte flow velocity, which improves bubble removal, while maintaining a low-pressure drop between the cell inlet and outlet. Figure 15a provides the CFD simulation results of the velocity field comparison between selected different flow channels. In addition, the modelled current-voltage (IV) curve comparison for the FEC (Figure 15b), derived from the different flow channel designs, shows the proposed new flow channel design significantly improves FEC performance. Further FEC structure optimisation could be implemented based on the developed CFD model.

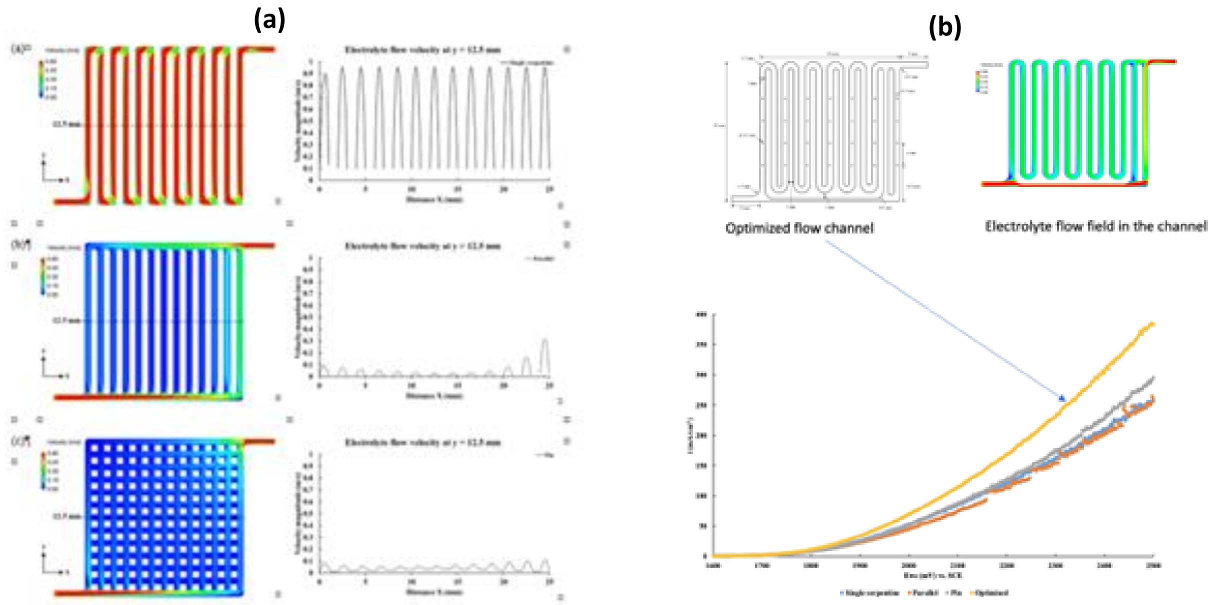

Figure 15: *(a) CFD modelling of various potential flow channel configurations within the FEC; (b) Optimum channel configuration (top) is shown based on the IV curve performance (bottom).*

3. Challenges Encountered and Lessons Learned

3.1 Biomass Pretreatment Reactor

(i) Challenge: *Reactor pressure increase upon heating.* The solar thermal BPR is run using a semi-batch operation where reaction temperature (120-150°C) leads to an internal pressure increase (1-6 Bar) in the reactor. Fittings and seals must be able to accommodate the increased operating pressure and temperature. The solar thermal BPR is an evacuated solar tube (see Figure 7, comprising borosilicate glass with an outer/inner tube diameter of 58/47mm and wall thickness of 1.6mm) and less tolerant to pressure (internal pressure limit is 10 Bar). Rupture of seals/fittings or breakage of glass could lead to release of the reaction fluid (sulfuric acid at pH 1-3) which is a significant hazard.

Resolution: The solar thermal BPR was reconfigured to contain a C20 stainless-steel vessel within the evacuated glass tube, which is more tolerant to high pressure, such that the reaction fluid is completely contained. Seals/fittings used in the reactor array are tolerant to elevated pressures and temperatures, and a pressure release valve has also been fitted to the reactor array to ensure operational safety.

(ii) Challenge: *Exposure of the reactor to environmental elements.* The primary component of the solar thermal BPR is an evacuated tube collector (supplied by our **Industry Partner** Apricus Australia). The glass has a lower thermal expansion coefficient (3.3 x 10^{-6} K^{-1}) compared to stainless-steel (17.2 x 10^{-6} K^{-1}). The different degrees of thermal expansion of the different material can lead to glass breakage when exposed to environmental elements over time and the accompanying temperature fluctuations (advice and experience provided by Apricus CEO, Mick Humphries). Breakage could lead to release of reaction fluid (sulfuric acid at pH 1-3) which is a significant hazard. Further, breakage will considerably increase material, operational and maintenance costs.

Resolution: The solar thermal BPR was reconfigured to contain a C20 stainless-steel vessel within the evacuated glass tube such that reaction fluid is completely contained if the outer glass tube breaks. Moreover, re-designed Teflon gaskets/O-rings/aluminum fin were added between the evacuated solar tube and stainless-steel components (end cap and vessel). Consequently, the thermal expansion of the stainless-steel components can be absorbed/accommodated by redesigned fittings, making the biomass reactor resistant to thermal shock. A spill tray is also located below the reactor to capture and contain any leaks.

(iii) Challenge: *Need for acidic conditions for biomass preconditioning process in solar thermal BPR.* The biomass preconditioning process requires an acidic environment (sulfuric acid at pH 1-3) within the solar thermal BPR. This is undesirable from a commercial viewpoint as working with volumes of acid at elevated temperature (e.g., 120-150°C) represents a significant hazard.

Resolution: Two possible solutions are using neutral conditions (i.e., pH ~7) in the BPR or a solid acid catalyst in place of the sulfuric acid. Commercially available solid acid catalysts, such as zeolite ZSM-5, may be appropriate with the intent being to work on this in future activities.

3.2 Flow Electrolyser Cell

(i) Challenge: *Maintaining uniform coating of active catalyst on electrode surface with increasing electrode size.* To improve the efficiency of hydrogen generation in the electrocatalytic cell, the standard nickel foam electrodes were modified by coating with a

NiMo alloy. The NiMo alloy was coated using a standard electrodeposition process. For the initial laboratory-scale studies, small Ni foam electrode sizes (i.e., 1.0 × 1.0, 2.0 × 2.0, 3.0 × 3.0 cm^2) required coating. The prototype FEC system employs larger-sized Ni foam electrodes (~8.0 × 8.0 cm^2) in the unit whereby obtaining a uniform coating of the NiMo alloy at this scale proved to be far more challenging. A non-uniform coating of the NiMo alloy had a negative impact on electrode performance.

Resolution: To provide a more uniform NiMo coating on the larger Ni-foam electrodes, the electrocatalytic array design used in the prototype FEC system was adapted to the coating process (Figure 16). That is, the NiMo precursor solution was passed through cathodic compartment of the cell and 1M KOH passed through the anodic compartment of the cell to impose the NiMo alloy coating.

Figure 16: *Flow electrode cell set-up for coating NiMo alloy on larger-scale Ni foam electrodes.*

(ii) Challenge: *Leaking of solution from the electrocatalytic cell.* Compared to small-size FECs (i.e., 1.0 × 1.0, 2.0 × 2.0, 3.0 × 3.0cm^2), the pressure drop across the inlet and outlet of a large-size FEC (8.0 × 8.0cm^2) during operation is greater, increasing by more than 100 kPa. The high pressure within the larger FEC in conjunction with the vigorous hydrogen bubble release can promote electrolyte leakage especially during long-term operation. The leaked alkaline electrolyte will lead to short circuiting of the FEC during operation, corrosion of metal components and wires, and is a safety hazard.

Resolution: To prevent leakage the FECs were redesigned to have a much more secure configuration. Modifications included optimizing the shape and size of the flow channels to ensure a low pressure drop and the smooth flux of the circulated electrolyte. New customised silicone gaskets, which are sandwiched between the electrodes and the graphite plate, were designed and fabricated to prevent the electrolyte from leaking through any corners. A revised array of eight nuts/bolts is now applied to firmly compress the FECs components and seal electrolyte within the cell.

3.3 Unit Coupling

(i) Challenge: *Ensuring the waste biomass feed stream is suitable for use in the Biomass Pretreatment Reactor and Flow Electrolyser Cell.* Studies on the system primarily used a control sugar solution to assess system performance. The control solution comprised a simple mixture of sugar in ultrapure water. In a real-world scenario, the feed to the BPR will contain other components such as suspended solids, bacteria, coloring and flavoring agents, preservatives (e.g., phosphoric acid), and mineral salts, etc. and will require some form of pre-treatment to facilitate long-term operation of the BPR and FEC.

Resolution: A waste biomass concentrator (WBC) arrangement was designed and installed upstream of the BPR to pre-treat more realistic feedstocks to be used by the tandem system. The WBC comprises: (i) a 5g/L activated charcoal suspension (25°C agitated at 200rpm); (ii) a ceramic ultrafiltration (UF) module (Filtanium Ceramic Membrane, 100KD, 0.004m^2 surface area, 10mm OD x 250 mm length); and (iii) a primary reverse osmosis module (RO1, PCI Polyamide Thin-Film Composite membranes, 0.2m^2 membrane area, 12.5mm OD × 600mm length, 9 piece/module); and a secondary RO module (RO2, Filmtec TW30HP-4611, Polyamide Thin-Film Composite membranes, 2.0m^2 membrane area/module). Performance of the WBC for treating a simulated soft drink waste stream is described earlier in Section 2.2. The concentrated sugar water feedstock with improved quality (>99% suspended solids, bacteria, and pigment removed) and significantly reduced volume, is a more economical/suitable feed for the solar-thermal BPR. The selective removal of inorganic ions is still to be investigated (and is intended as planned future work) as the presence of these ions may impose positive (increased conductivity) or negative (scaling issues) effects during the ensuing FEC stage.

(ii) Challenge: *The product from the Biomass Pretreatment Reactor is suitable as a feed for the Flow Electrolyser Cell.* The output stream from the solar thermal BPR is at temperature ranging between 120-150°C and is acidic in nature (pH 1-3) due to the requirement of sulfuric acid as an (homogeneous) acid catalyst. The characteristics of the post-BPR stream have to be appropriate for safe and effective operation of the FEC. Directly injecting the hot (> 80°C) acidic BPR output stream into the FEC will readily corrode the anodic electrode (designed to be stable in alkaline conditions). The elevated temperature may also increase the pressure inside the FEC and expand/loosen tube connections potentially leading to electrolyte leakage.
Resolution: A pre-conditioning reservoir, located between the BPR and FEC, was integrated into the system to adjust the BPR outlet stream characteristics to be suitable for the FEC. The BPR solution can be alkalified to a desired pH value (e.g., 14) suitable for injection into the FEC. There also exists the opportunity to recover some of the waste heat from the BPR to improve FEC system performance. Initial laboratory-scale optimisation studies indicated that an elevated FEC operating temperature (up to 60°C) provided improved unit performance. Future studies intend to modify the system to be able to harness waste heat from the BPR (operating temperature 120-150°C) to pre-heat the FEC feed and further improve system solar-to-hydrogen efficiency.

3.4 CFD Modelling

(i) Challenge: In an operating electrolyser the gas bubbles in the flow channel resulting from the OER/HER reactions cause a significant decline in efficiency. This problem becomes serious when the electrode has a higher performance. The bubbles coalescence inside the flow channel leading to blockages which affect electrical conductivity of the system. Solving this problem requires a combination of material development and FEC structure optimisation.
Resolution: A comprehensive CFD model as developed to describe the complicated electrolysis reactions in the lab-scale FEC. This model was validated against experimentally measured data and used to investigate the fluid dynamics inside the FEC. Based on the developed model, an optimised flow channel design was proposed to lower the bubble resistance in the FEC (Figure 15b). The numerical trials illustrated the mechanism behind the impacts of flow channel design adjustment on bubble removal efficiency. The optimal design can better control the pressure drop and electrolyte velocity with future experimental tests planned to verify the validity of the newly proposed design. The established numerical model can now be extended to investigate the impact of other structural improvements on FEC performance.

(i) Challenge: Modelling the FEC performance using various electrolytes, i.e., 5-HMG and BPR output solution, is difficult as they are multi-component liquid mixtures, and the electrolysis reactions are more complicated than for water splitting (i.e., OER and HER). Further, the generated by-products from electrolysis may affect electrode efficiency, leading to increasingly diminished accuracy of the simulation.

Resolution: Defining the complicated 5-HMF/BPR output electrolysis reactions in the numerical model requires species characterization from experimental studies. The experimental trials could also provide information regarding the relationship between electrode performance and electrolyte adjustment. Such impacts could then be described by mathematical models and be coupled in the CFD model. Consequently, the integration of experimental and numerical works is needed to resolve the issue, which will require substantiative trials to conclude the mechanism.

4. Commercialisation Prospects

Primary project outcome: A working stand-alone prototype array suitable for roof-top operation/studies and technology/concept demonstration purposes. The technology was progressed from TRL3 to TRL4 over the course of the project. Currently, the prototype system can produce 96 L H_2 per day (0.067 L H_2/min) from 25 L/day of waste sugar feedstock (~5 g/L sugar concentration).

Commercial interest: Following the 1st Rio Tinto – UNSW Forum (held on-line 15/02/2022) and a follow-up visit to UNSW (on 15/06/2022) by the Rio Tinto Chief Scientist and members of his Office, Rio Tinto saw potential in adapting the technology to their remote mining communities. Subsequently, ~$2M AUD has been provided to fund a new four-year project between UNSW and Rio Tinto within the NSW Trailblazer Program with the goal of progressing the technology from TRL4 to TRL6/7. The intent of the new collaboration is to integrate the technology into the management of organic-containing waste stream(s) in remote communities to value-add to the existing process(es). Added value will be in the form of renewable hydrogen generated from the waste stream for subsequent use (e.g., as a clean energy source) and the potential for improved waste quality (e.g., simpler and less-costly handling/management, less toxic). The project is due to commence in early 2023.

Pathway to commercialisation: Currently the technology lies at TRL4.The next stage involves adapting the technology to a real-world situation. This will be realised in collaboration with Rio Tinto (through the Trailblazer Program mentioned above) for example, at one of their remote mining sites located in the Pilbara. It is envisaged that the technology will initially be usable by small communities in remote and rural locations and will be in the form of modular and mobile systems. Pending the outcomes from identifying the suitability of the unit for the Rio Tinto test case scenario, the technology may be adapted to other Rio Tinto sites and/or other diverse local/remote communities, initially nationally and then internationally.

5. Knowledge-Sharing Activities

The following lists the activities undertaken and outputs arising from the Activity.

5.1. Events/Activities/Outreach

(1) 20/07/2022: Visit by CSIRO Chief Scientist, Dr Larry Marshall, and colleagues to UNSW laboratories where the concept/technology was viewed/explained.

(2) 15/06/2022: Visit by Rio Tinto Chief Scientist, Dr Nigel Steward, and members of the Rio Tinto Office of the Chief Scientist to UNSW laboratories where the concept/technology was demonstrated (roof-top).

(3) 26/05/2022: Visit by German Minister for Education and Research, Ms Bettina Stark-Watzinger, and HySupply delegation to UNSW including tour of UNSW laboratories where the concept/technology was demonstrated on the Tyree Energy Technology Building roof-top (Figure 17).

Figure 17: *Roof-top demonstration of tandem biomass system to German Minister for Education and Research (left) and HySupply delegation (right) on 26/05/2022.*

(4) Oct 2021 – current: On invitation by Dr Peter Grubnic, CI Scott joined the CSIRO HyResearch Steering Committee to assist with developing a live online portal detailing prior (since 2018) and ongoing hydrogen research within Australia across the entire value chain. Phase 1 of the HyResearch Portal (Projects) was officially launched in December 2021 with Phase 2 of the HyResearch Portal (Capability) officially released in September 2021. The HyResearch Portal can be found at https://research.csiro.au/hyresearch/.

(5) 18-20 October 2021: CI Scott Chaired the 4th Energy Future Conference (EF4) which was a completely online event hosted by UNSW Sydney, Australia. The conference discussed emerging technologies across the hydrogen value chain from hydrogen production and conversion, storage, distribution, safety and standards, applications, as well as unseen challenges associated with establishing the Hydrogen economy including environmental issues, water supply and social acceptance. It was attended by over 100 (registered) delegates and included invited presentations by representatives from the other ARENA-funded projects on Renewable Hydrogen for Export. Details on EF4 can be found at https://www.ausenergyfuture.com/.

(6) July 2020: Ph.D. student William Hadinata Lie (externally funded Ph.D. stipend) participated in the UNSW Three Minute Thesis (3MT) competition, describing his work on

the FEC component of the project. He was nominated as the best presentation from the UNSW School of Chemical Engineering.

(7) 06/02/2020: CI Scott attended CSIRO Hydrogen Industry Mission Briefing, in Melbourne. Subsequently, on 11/03/2020, CI Scott submitted an Expression of Intent (with CI Amal and Prof. Aguey-Zinsou (UNSW)) in support of the CSIRO Hydrogen Industry Mission.

(8) May-Dec 2019: CI Scott, on invitation from Dr Vivek Srinivasan (CSIRO Futures Group), joined CSIRO Hydrogen RD&D Opportunities Steering Committee to assist with generating CSIRO report: "Hydrogen Research, Development and Demonstration: Opportunities and Priorities for Australia." Report was released in December 2019 and can be found at www.csiro.au/en/Showcase/Hydrogen. CI Scott attended the report launch in Melbourne 05/12/2019.

(9) 16/05/2019: CIs Scott, Wang, Bedford and Amal met with Dr Max Temminghoff and Dr Vivek Srinivasan from CSIRO Futures Group. Delivered presentation outlining concept of ARENA Waste Biomass to Renewable Hydrogen project.

(10) 29/07/2019: CEO of Apricus Energy (Victoria-based Industry Partner), Mick Humphreys, participated in the Biomass Project Team meeting (face-to-face).

(11) 18/12/2019: CIs Scott and Wang met with Chris Williams and Steve Ward from Canvas Events (www.canvasevents.com.au) to discuss renewable hydrogen technologies at UNSW (including the ARENA project).

(12) 26/06/2019: All CIs met with Ken Baxter (Energy Advisor, Innovation and Partnerships) and colleagues from Melbourne Water via video link. Melbourne Water was interested in extracting hydrogen from their municipal waste sludge streams and reached out after seeing the project on the ARENA website.

(13) 24/05/2019: CIs Scott and Taylor met with delegation from Nanjing Tech University (China) where details on the project were presented.

5.2. Journal Publications

Published

(1) Jiang, L., Pan, J., Li, Q., Han, C., Zhou, S., Yu, Z., Jiang, S., Yin, H., Guan, J., Taylor, R.A., Fisher, R., Leslie, G., Scott, J., Zhao, H., Wang, D., A holistic green system coupling hydrogen production with wastewater valorisation, *EcoMat*, e12254 (2022).

(2) Li, Q., Charlton, A.J., Omar, A., Dang, B., Le-Clech, P., Scott, J. and Taylor, R.A., A novel concentrated solar membrane-distillation for water purification in a building integrated design, *Desalination*, 535, 115828 (2022).

(3) Li, Q., Zhuo, Y., Shanks, K., Taylor, R.A., Conneely, B., Tan, A., Shen, Y., Scott, J., A winged solar biomass reactor for producing 5-Hydroxymethylfurfural (5-HMF), *Solar Energy*, 218, 455-468 (2021).

(4) Hadinata Lie, W., Deng, C., Yang Y., Tsounis, C., Wu, K.H., Chandra-Hoe, M.V., Bedford, N.M., Wang D.-W., High yield electrooxidation of 5-hydroxymethyl furfural catalysed by unsaturated metal sites in CoFe Prussian Blue Analogue films, *Green Chemistry*, 23, 4333-4337 (2021).

In Preparation

(1) Li, Q., Jiang, L., Huang, G., Wang, D.-W., Markides, C.N., Taylor, R.A., Scott, J., Full spectrum solar utilization for generating renewable hydrogen from a waste biomass feedstock.
(2) Yang, Y., Scott, J., Bedford, N., Defect-rich ultrathin Ni-based LDH with high deprotonation capability for facilitating 5-HMF oxidation reaction kinetics.
(3) Yang, Y., Scott, J., Bedford, N., Stimulated hydrogen evolution and 5-HMF oxidation reactions on NiFe@MoS_2 bifunctional catalyst by M-O-M centre-mediated PECT process.
(4) Zhuo, Y., Jiang, L., Li, Q., Wang, D., Shen, Y., Scott, J., An integrated experimental and numerical study of the alkaline water electrolysis in a lab-scale electrolyser.

5.3. Social Media/Conferences/Workshops

(1) Li, Q., Scott, J., 'Waste Biomass to Renewable Hydrogen: ARENA Advancing Renewables Program.' Promotional video. Follow link https://www.pcrg.unsw.edu.au/waste-biomass-to-renewable-hydrogen.
(2) Taylor, R., IEA SHC Task 69: Smart Solar Water Heating for 2030, 2022 Asia Pacific Solar Research Conference, 29 Nov. – 1 Dec. 2022, Newcastle, NSW, Australia.
(3) Taylor, R., UNSW Solar Thermal Research Overview, ISES and IEA SHC International Conference on Solar Energy for Buildings and Industry (Eurosun 2002), 25-29 September 2022, Kassel, Germany.
(4) Jiang, L., A Holistic Green System Coupling Hydrogen Production with Wastewater Valorisation, 2022 International Symposium on Clean Energy Materials (ISCEM2022), 30 June – 2 July 2022, Gold Coast, Qld, Australia.
(5) Yang, Y., Scott, J., Bedford, N., Dynamically Structure-Evolved Ultrathin Layered Double Hydroxide Nanosheets for Highly Efficient 5-(hydroxymethyl)furfural Oxidation, 2022 MRS Spring Meeting & Exhibit, 8-13 May 2022, Honolulu, Hawai'i.
(6) Amal, R., Scott, J., Dai, L., Session 1: Carbon utilisation (circular carbon economy) for decarbonization, 1st Rio Tinto – UNSW Forum (on-line), 15 Feb. 2022.
(7) Li, Q., Development of A PV/Thermal Solar Collector for Transforming Waste Sugar to Hydrogen, 4th Energy Future Conference (EF4 2021) 18-20 Oct. 2021, Sydney, NSW, Australia.
(8) Scott, J., Renewable hydrogen from waste biomass: Value-adding to the water electrolysis process, Second International Forum on Hydrogen Production Technologies (HyPT-2), Sept 14-16, 2021.
(9) Scott, J., Renewable hydrogen generation and chemical storage: Value-adding to the process, Kobe City Government - UNSW online event, 24 June 2021.
(10) Scott, J., Renewable Hydrogen from Waste Biomass, ARENA Hydrogen R&D Roundtable Webinar, hosted by Melbourne Energy Institute (online), 17 -18 Feb. 2021.

6. Conclusion and Future Plans

6.1 Conclusion

A stand-alone, scalable prototype system capable of generating renewable hydrogen from a simulated biomass solution using only sunlight, that is more efficient than conventional water splitting, has been established. The system comprises three principal components: (i) a waste biomass concentrator to concentrate the organic waste feed stream (for use in the solar-thermal biomass pre-treatment reactor) and simultaneously produce clean water (for use in the flow electrolysis cell); (ii) a solar-thermal biomass pre-treatment reactor for pre-conditioning the concentrated organic waste stream; and (iii) a photovoltaic-powered flow electrolysis cell to produce renewable hydrogen. The system does not emit CO_2 and has the capacity to derive value-added products from the waste biomass stream. In terms of development and performance, the prototype system:

(i) can produce 96 L H_2 per day (0.067 L H_2/min) from 25 L/day from a 'control' waste sugar feedstock (~5 g/L sugar concentration);

(ii) progressed from TRL3 to TRL4;

(iii) can convert a maximum of ~58% solar energy to heat and electricity (50% solar to thermal efficiency at 150°C and ~ 8% PV efficiency);

(iv) can recover > 95% of sugar the wastewater and deliver <10 kWh/m^3 energy consumption for clean water production;

(v) offers an energy consumption of 40-54 kWh/kg of hydrogen using the output from the solar-thermal reactor (pre-conditioned sugar stream) in conjunction with an in-house-developed NiMo electrocatalyst. The energy consumption is 15% more efficient than traditional water splitting using a Ni foam electrocatalyst.

Further, new, validated predictive analysis tools, in the form of Computational Fluid Dynamic models, have been developed for the solar-thermal biomass pre-treatment reactor and photovoltaic-powered flow electrolysis cell units. The models allow for greater understanding of the phenomena occurring within both systems (e.g., BPR: temperature profile, product evolution profile; FEC: hydrogen/oxygen produced (from water splitting), internal state of the hydrogen/oxygen mass fraction distribution in the flow channels, current potential distribution on electrode surfaces, electrolyte flow field, the bubble formation). The established models can also assist with optimising design and operational conditions for next-generation and scaled-up systems.

Outcomes from the Activity demonstrate the viability of the proposed approach and show that a waste biomass stream can be used as an effective and more efficient substitute for clean water to generate hydrogen renewably. The technology exhibits the potential for impact in circumstances where clean water availability and management is important, as well as provides an alternative waste management strategy for industries and communities seeking to adopt circular economy framework. The Activity has also shown that the technology is scalable which has implications from a commercialisation standpoint.

6.2 Future Plans

The following activities have recently been instigated to further progress the tandem unit technology as well as expand its potential use into other applications:

(i) A Ph.D. stipend has been awarded through the ARC Training Centre for the Global Hydrogen Economy to further evaluate and evolve the tandem unit. The intent of the PhD is to better understand the system with the generated understanding designed to progress it towards real-world applications (e.g., study real biomass-containing streams, impact of waste stream components (other than biomass) on performance, minimize need for acidification of biomass feed stream). As part of the Ph.D.: (i) a technoeconomic evaluation will be undertaken to determine technology viability from a cost-performance position and identify components within the system where cost reductions are needed; (ii) the models will be advanced to predict hydrogen generation from biomass waste streams (e.g., pre-treated sugar solution from the BPR) based on the experimental data generated during the Ph.D.

(ii) Through the NSW Trailblazer funding platform, ~$2M AUD has been committed to a joint project with Rio Tinto to further develop the biomass reforming technology established within this ARENA Activity. The goal of the collaboration is to progress the technology from TRL4 to TRL6/7 by integrating the tandem unit into the organic waste management process at a remote Rio Tinto mining location. The new project is expected to commence in early 2023.

(iii) Opportunities for adapting the tandem unit concept to other applications have been sought. In this regard, a collaborative effort has been established between the UNSW School of Chemical Engineering and FP Paradigm Pty Ltd to transition the current food packaging standard of transparent petroleum-based material into transparent non-petroleum based sustainable material with smart sensing capabilities. The collaboration is being supported via the Australian Government AusIndustry funding program, to the value of ~$2.5M over three years. The activity is centered on the idea of a tandem solar-thermal reactor/flow electrolytic cell array (i.e., process concept inspired by this ARENA project) for producing the transparent packaging material using green chemistry. The project is due to commence in late 2022.

Appendix

Table A1. *Characteristics of sugar wastewater feedstock and product water as it passes through the waste biomass concentrator (WBC) array. Also provided are typical sugar-containing wastewater characteristics and values from industrial soft-drink manufacturing processes as reported in the literature.*

Characteristics	**Sugar wastewater from literature**	**Activated charcoal + UF**		**RO (feed is permeate from UF process)**	
		Feedstock	Permeate	Conc. Feed	Permeate
	Number in Fig 2	1	2	3	4
pH	3.4 - 12[1,3,4]	3.38	2.98	3.10	4.30
Conductivity (µS/cm)	266 - 1,483[1,3]	357	538	766	52
Colour (absorbance 466-610nm)	Dark yellow	0.094-0.035	0.001-0.004	0.075-0.109	0.025-0.035
Sugar (fructose and sucrose) (mg/L)	1,350 - 7,972[1]	1° Brix (10 g/L)	1° Brix (10 g/L)	2° Brix (20 g/L)	0.1° Brix (1 g/L)
Viscosity at 20°C (mPa s)	0.72-1.5 (5 - 20 wt% sugar content)	1.2	1	1.5	1
COD (mg/L)	1,616 - 15,000[1-4]	/	/	/	/
TOC (mg/L)	1,987[3]	4025	3922	7207	213
Total nitrogen (mg/L)	22 - 49[4] 20 - 1,180	16.5	14.2	20.2	0.27
Total phosphorus (mg/L)	4 - 13[4] 130 - 250	/	/	/	/
Phosphate (mg/L)	1.2 - 8.8[1]	27.5	110	326	12.9
CO_3 and HCO_3 (mg/L)	168 - 662[1,3]	41	41.5	55.5	90
Sulphates (mg/L)	5.0 - 20.8[1]	/	/	/	/
Calcium ions (mg/L)	13 - 25[1]	2.21	1.8	5.26	0.1-0.34
Sodium ions (mg/L)	83 - 183[1]	2.49	3.3	9.55	0.25-0.32
Chloride ions (mg/L)	20 - 45[1]	2.63	2.6	3.23	1.92

Note: COD - chemical oxygen demand; TOC- total organic carbon.

References

[1] Sheldon, M.S., Erdogan, I.G., Multi-stage EGSB/MBR treatment of soft drink industry wastewater, *Chem. Eng. J.*, 285, 368-377 (2016).
https://doi.org:https://doi.org/10.1016/j.cej.2015.10.021

[2] Güven, G., Perendeci, A., Tanyolaç, A., Electrochemical treatment of simulated beet sugar factory wastewater, *Chem. Eng. J.*, 151, 149-159 (2009).
https://doi.org:https://doi.org/10.1016/j.cej.2009.02.008

[3] Durán, A., Monteagudo, J.M., Gil, J., Expósito, A.J., San Martín, I., Solar-photo-Fenton treatment of wastewater from the beverage industry: Intensification with ferrioxalate, *Chem. Eng. J.*, 270, 612-620 (2015).
https://doi.org:https://doi.org/10.1016/j.cej.2015.02.069

[4] Peixoto, G., Saavedra, N.K., Varesche, M.B.A., Zaiat, M., Hydrogen production from soft-drink wastewater in an upflow anaerobic packed-bed reactor. *Inter. J. Hydrogen Energy*, 36, 8953-8966 (2011).
https://doi.org:https://doi.org/10.1016/j.ijhydene.2011.05.014